A Letters Journal Exploring the Frontiers of Physics

December 2014

EPL, **108** (2014) 67012
doi: 10.1209/0295-5075/108/67012

www.epljournal.org

Giant electronic polarization induced by a helical spin order in $SrMn_7O_{12}$: First-principles calculations

H. M. Liu[1], Shuai Dong[2(a)], Z. Z. Du[1], P. Chu[1] and J.-M. Liu[1(b)]

[1] *Laboratory of Solid State Microstructures and Innovation Center of Advanced Microstructures, Nanjing University - Nanjing 210093, China*
[2] *Department of Physics, Southeast University - Nanjing 211189, China*

received on 4 December 2014; accepted by S. Savrasov on 11 December 2014
published online 7 January 2015

PACS 71.20.-b – Electron density of states and band structure of crystalline solids
PACS 75.85.+t – Magnetoelectric effects, multiferroics
PACS 77.80.-e – Ferroelectricity and antiferroelectricity

Abstract – Through first-principles density functional calculations, the magnetic ground state and electronic structure of mixed-valent manganite $SrMn_7O_{12}$ in the rhombohedral symmetry are investigated in detail. Our calculations show clearly that the possible magnetic ground state accommodates a particular helical spin order responsible for the insulating state in $SrMn_7O_{12}$. The giant ferroelectric polarization is revealed, which is almost purely from the electronic contribution rather than the ionic displacements and is closely related to the magnetism. The influence of the on-site Coulomb interaction and spin-orbit coupling on the electronic structure and multiferroicity is also discussed. The present results suggest that $SrMn_7O_{12}$ is a promising multiferroic candidate with desirable properties.

Introduction. – Single-phase multiferroic compounds in which magnetism and ferroelectricity coexist have been a new surge of interest because of the fundamental importance of the magnetoelectric (ME) effect and potential technological applications. A number of magnetic multiferroics or so-called type-II multiferroics, whose polarizations are caused by particular spin orders, have been discovered, taking $TbMnO_3$ [1,2] and $MnWO_4$ [3,4] as two representative examples with the cycloidal spin order responsible for the ferroelectricity generation. The origin of ferroelectric (FE) polarization in these compounds can be described by the inverse Dzyaloshinskii-Moriya (DM) interaction [5], or the spin current model [6]. However, their FE polarizations tend to be quite small (mostly lower than $1000\,\mu C/m^2$) and the Néel temperatures are low (mostly below 40 K). These disadvantages can be partially overcome in exchange striction dominant multiferroics such as the E-type antiferromagnetic (AFM) manganite $HoMnO_3$ which possesses a big polarization up to the magnitude of order of $10000\,\mu C/m^2$ [7,8]. Nevertheless, the FE Curie temperatures (T_c's) in these materials remain low (~ 30 K) either [9].

Recently, the mixed-valent manganite $CaMn_7O_{12}$ with a helical magnetic structure was found to exhibit a giant FE polarization up to $2870\,\mu C/m^2$ along its c-axis since 90 K [10,11]. More interestingly, the magnetic structure uncovered so far disobeys the conventional inverse DM interaction model [5] or the spin current model [6] for the induced ferroelectricity in which the polarization is constrained on the plane of spin rotation. In $CaMn_7O_{12}$, the polarization is perpendicular to the spin rotation plane. To understand the microscopic origin of this giant polarization in $CaMn_7O_{12}$, a phenomenological ferroaxial coupling mechanism was proposed recently [11,12]. Then, it was suggested that the magnitude of polarization is mainly governed by the exchange striction while its direction is determined by the chirality of the helical spin structure due to the strong DM interaction [13]. This is the first case other than the conventional models, in which the magnitude and direction of the polarization are dominated by separated mechanisms although both are spin order related.

In parallel, an interesting question is whether $CaMn_7O_{12}$ is unique? It would be of specific significance to search for more magnetic multiferroics in the big quadruple perovskite family. Some of the authors

(a) E-mail: sdong@seu.edu.cn
(b) E-mail: liujm@nju.edu.cn

once predicted the multiferroic phases in quarter-doped narrow-bandwidth manganites [14]. There is no reason to limit our eyes only to $CaMn_7O_{12}$. In this work, we intend to investigate $SrMn_7O_{12}$, the first neighbor of $CaMn_7O_{12}$. Our main motivation is based on the following facts. First, at low temperatures (T's), $SrMn_7O_{12}$ shares the same rhombohedral structure (space group $R\bar{3}$) with the ferroelectrically polarized $CaMn_7O_{12}$. Second, the Sr^{2+} ion is quite larger than the Ca^{2+} ion, which may enable a different lattice distortion of $SrMn_7O_{12}$ from that of $CaMn_7O_{12}$. Therefore, the ferroelectricity and magnetic ground state of $SrMn_7O_{12}$ in terms of its difference and similarity with $CaMn_7O_{12}$ would be of particular significance. Third, $SrMn_7O_{12}$ has already been synthesized as early as in 1974 [15], yet rarely its magnetic and electronic properties have been studied due to the high-pressure synthesis conditions. Our calculations may provide a promising verification in order to perform more careful investigations on $SrMn_7O_{12}$ experimentally. No need to mention that these issues also make a reliable theoretical prediction of the multiferroic properties quite challenging.

In this work, on the basis of the full-scale first-principles density functional theory (DFT) calculations, we shall reveal that $SrMn_7O_{12}$ can be a promising magnetic multiferroic candidate with a giant ferroelectric polarization which is intrinsically related to the magnetic order and electronic structure. More interesting is that this compound is a novel member in the category of magnetic multiferroics in which electronic polarization is much dominant over the ionic displacement contribution. The remaining parts of this paper are organized as follows. The procedure of the first-principles calculations for this compound is given in the next section. The main results and discussion on the electronic structure, spin order, and ferroelectric behavior are presented in the third section. The impact of the spin order and on-site Coulomb interaction U as well as spin-orbit coupling (SOC) on the electronic structure and ferroelectricity will be investigated in detail. This work will be concluded in the last section.

Method. – Our first-principles calculation is performed using the VASP (Vienna *ab initio* simulation package) code [16,17] and the GGA (generalized gradient approximation) PBE (Perdew-Becke-Erzenhof) function [18]. The PAW (projector augmented-wave) pseudopotential [19] is utilized with a plane-wave energy cutoff at 450 eV. A unit cell containing three chemical units with 60 atoms is adopted, and k-points sampled using a $2 \times 2 \times 3$ Monkhorst-Pack mesh are used. The influence of U and SOC will be taken into account in the present study.

For the calculation consideration, we note that $SrMn_7O_{12}$ belongs to the quadruple $(AA'_3)B_4O_{12}$ family. There are three different symmetry inequivalent sites for Mn ions which are labeled as Mn1, Mn2, and Mn3, respectively. The Mn1 ions occupy the sites of Wyckoff position 9*e* (0.5, 0, 0); Mn2 ions occupy the sites of Wyckoff position 9*d* (0.5, 0, 0.5); Mn3 ions occupy the Wyckoff position 3*b* (0, 0, 0.5). The Mn2 and Mn3 ions, which are both in the B-sites of perovskite structure, are in the mixed valence (+3.25) at high temperatures but become charge ordered as temperature decreases [20]. Therefore, the chemical formula of $SrMn_7O_{12}$ can be re-written as $Sr^{2+}(Mn^{3+})_3(Mn^{3.25+})_4O_{12}^{2-}$ or $Sr^{2+}(Mn^{3+})_3[(Mn^{3+})_3(Mn^{4+})]O_{12}^{2-}$ as well. A sketch of the lattice structure is presented in fig. 1(a), where the Sr, Mn1, Mn2, Mn3, and O ions are represented by blue, wine, yellow, green, and dark-yellow balls, respectively.

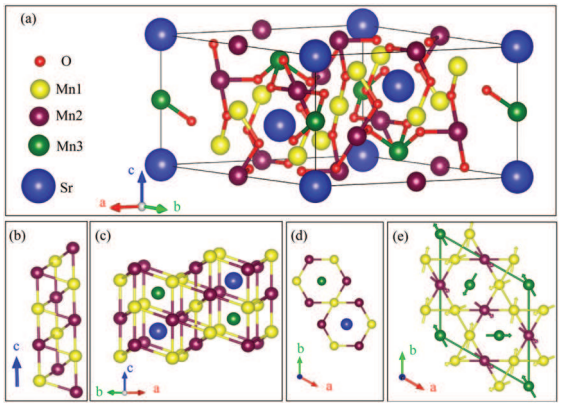

Fig. 1: (Colour on-line) (a) Structure scheme of rhombohedral $SrMn_7O_{12}$. The blue, wine, yellow, green and red balls are the Sr, Mn1, Mn2, Mn3 and O ions, respectively. (b) The schematic diagram of three adjacent chains of the Mn1 and Mn2 ions along the c-axis. (c) View of arrangements of the Sr ions and all the Mn ions from the side, the Sr and Mn3 ions are alternatively arranged in a line. (d) The projection of the stereogram in the c-direction. (e) The calculated magnetic structure of $SrMn_7O_{12}$ in the ab plane. Mn1, Mn2 and Mn3 ions and their spin directions are figured as wine, yellow and green arrows, the length of the spin arrows represents the magnitude of the magnetic moments.

In our calculation, in the first step, the crystal structure of $SrMn_7O_{12}$ in the rhombohedral symmetry is optimized. For this, the atom positions are fixed according to the experimental data [15] and the lattice constants are fully relaxed without including magnetism until the Hellmann-Feynman force acting on each atom is reduced down to 0.01 eV/Å. The lattice optimization is carried out with on-site Coulomb interaction $U = 3.0$ eV [18], and the Hund rule coupling factor $J_H = 1.0$ eV is fixed during the entire calculations. The optimized process provides the relaxed lattice constants: $a_0 = b_0 = 10.527$ Å, $c_0 = 6.391$ Å, in excellent agreement with the experimental estimation of $a_0 = b_0 = 10.509$ Å and $c_0 = 6.384$ Å [15].

Results. –

Magnetic ground state. Subsequently, we consider the magnetic structure. Since no clear experimental

Table 1: Energy differences (in unit of eV per unit cell) of three different situations compared with the non-magnetic state at different values of U (in unit of eV)

		$U = 1.5$	$U = 2.0$	$U = 3.0$	$U = 4.0$
Without SOC	FM	−37.598	−43.527	−54.641	−64.251
	AFM	−37.550	−43.288	−54.178	−63.635
	Helical	−38.147	−43.840	−54.683	−64.085
With SOC	FM	−38.044	−43.937	−55.026	−64.618
	AFM	−38.067	−43.798	−54.676	−64.126
	Helical	−38.668	−44.249	−55.182	−64.590

conclusion for $SrMn_7O_{12}$ has been available, several different spin orders, including the ferromagnetic (FM) order, helical spin order, and an antiferromagnetic (AFM) order, are tested here. The AFM state refers to the fact that all Mn1 spins are up and all Mn2/Mn3 spins are down. For the helical spin order, it is known that $CaMn_7O_{12}$ below 90 K adopts a complicated helical spin order with the propagation vector $k = (0,\ 1,\ 0.963)$ [11]. To reduce the computational task here, noting that the unit cell for the present calculation has 60 atoms, we start from the spin structure of $CaMn_7O_{12}$ with a slight modification of the propagation vector k, *i.e.* we choose a commensurate vector $k = (0,\ 1,\ 1)$. The Mn1 and Mn2 ions are arranged in a straight line along the c-axis and a schematic diagram is displayed in fig. 1(b). Figure 1(c) is a stereogram of the Sr ions and all the Mn ions, illustrating that the Sr ions and Mn3 ions are alternatively arranged in a line. For a better understanding of the structure, the stereogram projection along the c-axis is exhibited in fig. 1(d). It is seen that each Sr ion or Mn3 ion occupies the middle of a hexagonal which is made of six Mn^{3+} ions (three Mn1 and Mn2 ions each). The three contiguous Mn1-Mn2 ions form a triangle if one observes along the c-axis and the Mn^{3+} spins are nearly perpendicular to the c-axis. Therefore, each chain in fig. 1(b) is ferromagnetically ordered and these FM chains form a helical (spiral) spin order of 120° degrees in angle.

Now we perform the calculation for these spin orders given different values of U for revealing the magnetic ground state. The calculated results on these spin orders are listed in table 1. It is shown that the helical spin order has a lower energy than that of either the FM order or the AFM order at $U \leq 4.0$ eV, no matter whether the SOC effect in included or not. Regarding the choice of U value here, as revealed in earlier works [13,21,22], $U = 3.0$ eV is a proper value for manganites. This implies that the helical spin order is the magnetic ground state of $SrMn_7O_{12}$. Therefore, we take this value of $U = 3.0$ eV in the subsequent calculations unless mentioned otherwise. The calculated spin structure projected onto the ab plane is shown in fig. 1(e). As mentioned above, the Mn1, Mn2, and Mn3 spins are all nearly perpendicular to the c-axis, indicating the helical rotation plane on the ab plane. The

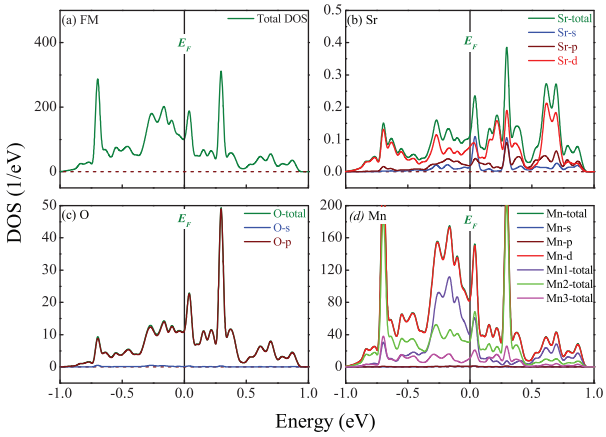

Fig. 2: (Colour on-line) (a) The total DOS patterns of non-magnetic $SrMn_7O_{12}$. (b) The partial DOS of Sr ions. The olive, blue, wine, and red lines represent the total, s-orbital, p-orbital and d-orbital DOS, respectively. (c) The partial DOS of O ions. The olive, blue, and wine lines represent the total, s-orbital and p-orbital DOS, respectively. (d) The partial DOS of Mn ions and 3d-total DOS of the Mn1, Mn2 and Mn3 ions. The olive, blue, wine and red lines represent the total, s-orbital, p-orbital and d-orbital DOS of Mn ions. The violet, green and magenta lines represent 3d-total DOS of the Mn1, Mn2 and Mn3 ions, respectively.

evaluated magnetic moments for the Mn1, Mn2, and Mn3 ions are $\sim 3.69\,\mu$B, $3.55\,\mu$B, and $2.93\,\mu$B, respectively.

Density of states. We then calculate the electronic structures of these spin orders by addressing the density of states (DOS). As a reference, we present in fig. 2 the calculated DOS without considering any spin order. While fig. 2(a) shows the total DOS, the individual contributions from the Sr, Mn, and O ions to the total DOS are plotted in figs. 2(b)–(d), respectively. In particular, the 3d orbitals DOS of Mn1, Mn2, and Mn3 ions are included in fig. 2(d). First of all, it is seen that $SrMn_7O_{12}$ is metallic with quite large DOS at the Fermi level if no spin moment is considered, as shown in fig. 2(a). Second, it is clear that the main contribution to the DOS around the Fermi level comes from the Mn ions, although the O-2p contribution cannot be ignored either. This implies the relatively strong p-d hybridization. Especially, the Mn1

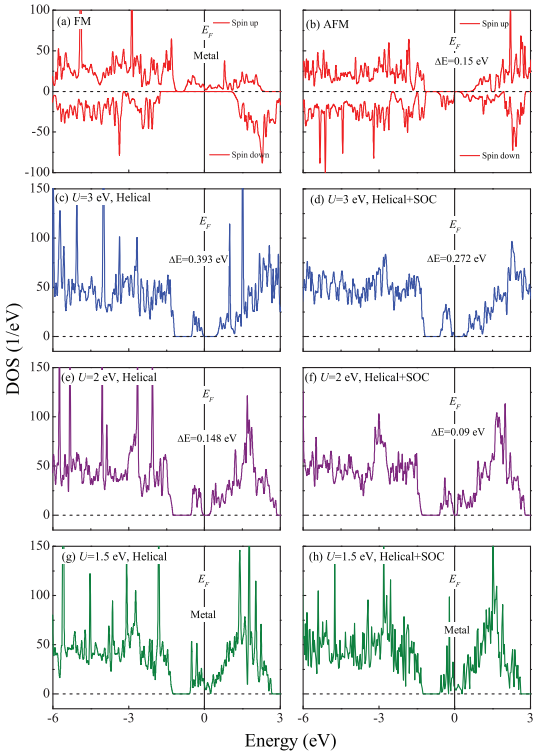

Fig. 3: (Colour on-line) (a) The total DOS patterns of (a) FM ordered $SrMn_7O_{12}$, (b) AFM ordered $SrMn_7O_{12}$. The total DOS of helical magnetic ordered $SrMn_7O_{12}$ using DFT + U calculations when (c) $U = 3\,\text{eV}$ without SOC. (d) $U = 3\,\text{eV}$ with SOC. (e) $U = 2\,\text{eV}$ without SOC. (f) $U = 2\,\text{eV}$ with SOC. (g) $U = 1.5\,\text{eV}$ without SOC. (h) $U = 1.5\,\text{eV}$ with SOC. The Fermi energy is chosen as zero.

and Mn2 ions have the dominant contribution, partially due to the fact that the number of Mn3 ions is only 1/3 of that for Mn1/Mn2 ions in each unit cell. Then we look at the electronic structures given different spin orders and the results are summarized in fig. 3. The detailed DOS data are presented in figs. 3(a)–(h). Figures 3(a) and (b) show the total DOS patterns of the FM order and AFM order. The DOS of helical spin order at different U values with or without SOC are plotted in figs. 3(c)–(h). According to fig. 3(a), the FM phase turns out to be a half-metal and the AFM phase is insulating with a gap of 0.15 eV in terms of fig. 3(b). For $U = 3.0\,\text{eV}$ without the SOC, the DOS calculations show a gap of 0.393 eV for the helical spin phase (fig. 3(c)). This gap reduces down to 0.272 eV if the SOC is included (fig. 3(d)). Upon U decreasing down to 2.0 eV, the gap decreases down to 0.148 eV without the SOC and 0.09 eV with the SOC, respectively, as shown in fig. 3(e) and fig. 3(f). When U is further reduced down to $U = 1.5\,\text{eV}$, finite DOS at the Fermi level appears and an insulator-metallic transition occurs even if the SOC is considered, as presented in fig. 3(g) and fig. 3(h), respectively.

The above results clearly state that for $SrMn_7O_{12}$ the magnetism can induce a metal-insulator transition. As displayed in fig. 2, the major components of the DOS

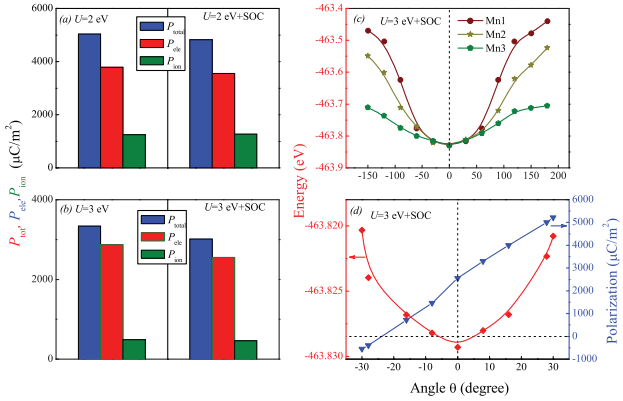

Fig. 4: (Colour on-line) (a) The total ferroelectric polarization, electronic and ionic contributions for different values of U, *i.e.*, (a) $U = 2\,\text{eV}$, (b) $U = 3\,\text{eV}$, with or without considering the SOC effect. The red, blue and olive areas represent the total, the electronic and the ionic polarization, respectively. (c) The total energy as a function of the Mn spin direction and the energy minimum occurs when $\theta = 0$. (d) Polarization and the total energy as a function of the Mn3 spin deviation.

around the Fermi level are from the Mn ions, and thus the magnetism of the Mn ion is the substantial origin for modulating the conductivity. This situation is reminiscent of the cross-coupling between the orbital order and spin order. For example, in colossal magnetoresistance (CMR) manganites, an orbital-ordered, insulating, and AFM state competes with a FM and isotropic metallic state, which can be controlled by the external magnetic field [23]. Recently, an orbital order in $CaMn_7O_{12}$, which is named as incommensurate magneto-orbital helix, was proposed [24]. In connection with our results on the relationship between the conductivity and spin order, one has reasons to believe that a similar orbital order may also exist in $SrMn_7O_{12}$.

Naturally, the gap between the conducting band and the valence band depends on U. Once the SOC is included, this gap is slightly reduced given the same U. Nevertheless, it is demonstrated that an insulating state with a sufficiently big gap is obtained for the helical spin order, which provides a pre-requisite for the ferroelectricity calculation to be shown below.

Polarization calculation. As stated above, the total polarization P is the sum of the ionic polarization P_{ion} and the electronic one P_{ele} [25]. To evaluate P_{ele}, the Berry phase method is adopted. For such calculations, the high-symmetry AFM phase is chosen as a reference state, noting that this AFM order preserves the inversion symmetry, thus free of any polarization. Our calculation shows that this AFM state is insulating and 0.32 eV per formula higher in energy than the helical spin state at $U = 3.0\,\text{eV}$. Starting from this state, the AFM order is replaced with the helical spin order with $k = (0,\ 1,\ 1)$, and then the atom positions are relaxed given the fixed lattice constants. The total polarizations are obtained by comparing the reference state and the polarized state.

The extensive calculations produce the data highlighted in fig. 4. We obtain P_{ele} by repeating the Berry phase calculation keeping the ionic positions frozen at their high symmetric phase by allowing the structure to adopt different magnetic states as AFM and helical spin states, and finally P_{ion} can be achieved by P_{tot} subtracting P_{ele}.

First of all, it is seen that $SrMn_7O_{12}$ offers a remarkable FE polarization P_{tot} and its magnitude is up to $\sim 5000\,\mu C/m^2$ ($U = 2.0\,eV$), comparable with and even larger than $CaMn_7O_{12}$. Second, it is shown that the polarization, both P_{ele} and P_{ion}, aligns along the c-axis, perpendicular to the helical spin rotation plane, similar to $CaMn_7O_{12}$ [13]. Third, the major contribution to the polarization is from the electronic component P_{ele} rather than the ionic component P_{ion} ($P_{ele} \gg P_{ion}$ and $P_{ele}/P_{tot} \sim 86\%$). These features demonstrate that $SrMn_7O_{12}$ is an attractive candidate of magnetic multiferroics and somehow more promising than $CaMn_7O_{12}$.

In detail, one has $P_{tot} = 3335.66\,\mu C/m^2$, $P_{ele} = 2869.46\,\mu C/m^2$ and then $P_{ion} = 486.20\,\mu C/m^2$ at $U = 3.0\,eV$ without the inclusion of the SOC effect. Given the SOC effect included with the optimized structure, one has $P_{tot} = 3012.95\,\mu C/m^2$, $P_{ele} = 2552.74\,\mu C/m^2$, and then $P_{ion} = 460.21\,\mu C/m^2$. It is seen that P_{ele} is slightly suppressed by the SOC effect. A similar case applies to different U. At $U = 2.0\,eV$, our calculations predict $P_{tot} = 5033.23\,\mu C/m^2$, $P_{ele} = 3788.81\,\mu C/m^2$, and then $P_{ion} = 1244.42\,\mu C/m^2$ if no SOC effect is taken into account. When the SOC is considered, the calculated $P_{tot} = 4820.09\,\mu C/m^2$, $P_{ele} = 3549.58\,\mu C/m^2$, and then $P_{ion} = 1270.51\,\mu C/m^2$. The electronic polarization associated with the SOC is $213.14\,\mu C/m^2$. These results show that the on-site Coulomb interaction has more prominent impact on the polarization than the SOC effect, while their roles are opposite.

Our calculations show that P_{ele} itself is one of the extraordinary phenomena in $SrMn_7O_{12}$. Here the total polarization is almost purely ($\sim 86\%$) electronic which is quite non-trivial even when comparing with other magnetic multiferroics. For example, the DFT calculations and experiments revealed that the electronic contribution to ferroelectric polarization is very limited (less than 10%) in bc spiral $TbMnO_3$ [2,22,26,27]. Even for the ab spiral $TbMnO_3$ and E-type AFM orthorhombic $HoMnO_3$, the DFT calculated results showed that the electronic contributions are about 60% of the total polarizations, which is larger than but still comparable to the ionic contribution [8,22,27,28]. The calculations reveal that the magnetic structure (spin order) and the possible orbital order (SOC effect) are the substantial ingredients of physics responsible for the ferroelectricity. Regarding the effect of U, it is understood that the decrease of U causes an impressive increase of P_{ele}, noting that P_{ele} mainly arises from the complex interactions in the helical spin-ordered state [13]. Due to the decrease of U in a certain reasonable range, the orbital overlap between the adjacent ions will be enhanced. Consequently, the spin interactions will be enhanced which eventually bring on an even larger electronic polarization.

Although the above calculations found that the helix spin order is the lowest in energy compared to the FM and AFM ones, it is better to further check the robustness of such a non-collinear spin order. Here the total energy of $SrMn_7O_{12}$ is recalculated by rotating three Mn's spins in the ab plane from the original helix one. As shown in fig. 4(c), the minimum of total energy appears at $\theta = 0$ (fig. 4(c)) for all three rotations, which confirms the robustness of the helix spin state. In ref. [13], it was found that in $CaMn_7O_{12}$, the spin orientation of Mn3 was mostly responsible for the strong ferroelectric polarization arising from the exchange striction and the ferroelectric polarization could be switched when changing the Mn3 spin direction as θ. Here, the ferroelectric polarization of $SrMn_7O_{12}$ as a function of a Mn3's spin changing path is calculated while Mn1 and Mn2 spins are unchanged. Within the small-θ region, the value of polarization depends almost linearly on θ (fig. 4(d)) which is consistent with the precious analysis about $CaMn_7O_{12}$ [13].

Such a giant P_{ele} governs the magnitude and even the direction of macroscopic polarization. The electronic response with little lattice deformations will promise both high-performance and high-frequency operations as well as rapid polarization switching against external perturbations. The remarkable polarization enhancement gives us a future way to search for better multiferroic materials. Surely, the SOC effect may be modulated by, *e.g.,* strain engineering or substitution of $4d$ or even $5d$ magnetic species.

Conclusion. – In summary, on the basis of the full-scale first-principles density functional theory calculations, we investigated the electronic structure and ferroelectric properties of $SrMn_7O_{12}$. The energy comparisons are performed with various U in the first place. It turns out that when U is in a reasonable region ($< 4\,eV$), the helical magnetic ground state is the same as that of $CaMn_7O_{12}$ obtained by neutron powder diffraction. Based on this, the electronic structures of $SrMn_7O_{12}$ are calculated. The magnetic orders have no doubt impacted the electronic structures and cause a metal-insulator transition which reveals the possible existence of the orbital order.

A giant improper ferroelectric polarization in $SrMn_7O_{12}$ which is parallel to the c-axis is induced by an in-plane helical magnetic structure according to our calculations. Most interestingly, the electronic polarization composes the majority ($\sim$86%) of the total polarization. And this ferroelectric polarization is mostly from the exchange striction effect instead of the spin-orbit coupling.

* * *

This work was supported by the Natural Science Foundation of China (11234005, 1374147 and 51322206), the National Key Projects for Basic Research of China (2011CB922101 and 2009CB623303), and the Priority

Academic Program Development of Jiangsu Higher Education Institutions, China.

REFERENCES

[1] Kimura T., Goto T., Shintani H., Ishizaka K., Arima T. and Tokura Y., *Nature*, **426** (2003) 55.
[2] Malashevich A. and Vanderbilt D., *Phys. Rev. Lett.*, **101** (2008) 037210.
[3] Taniguchi K., Abe N., Takenobu T., Iwasa Y. and Arima T., *Phys. Rev. Lett.*, **97** (2006) 097203.
[4] Tian C., Lee C., Xiang H., Zhang Y., Payen C., Jobic S. and Whangbo M. H., *Phys. Rev. B*, **80** (2009) 104426.
[5] Sergienko I. A. and Dagotto E., *Phys. Rev. B*, **73** (2006) 094434.
[6] Katsura H., Nagaosa N. and Balatsky A. V., *Phys. Rev. Lett.*, **95** (2005) 057205.
[7] Sergienko I. A., Sen C. and Dagotto E., *Phys. Rev. Lett.*, **97** (2006) 227204.
[8] Picozzi S., Yamauchi K., Sanyal B., Sergienko I. A. and Dagotto E., *Phys. Rev. Lett.*, **99** (2007) 227201.
[9] Ishiwata S., Kaneko Y., Tokunaga Y., Taguchi Y., Arima T. H. and Tokura Y., *Phys. Rev. B*, **81** (2010) 100411(R).
[10] Zhang G., Dong S., Yan Z., Guo Y., Zhang Q., Yunoki S., Dagotto E. and Liu J.-M., *Phys. Rev. B*, **84** (2011) 174413.
[11] Johnson R. D., Chapon L. C., Khalyavin D. D., Manuel P., Radaelli P. G. and Martin C., *Phys. Rev. Lett.*, **108** (2012) 067201.
[12] Mostovoy M., *Physics*, **5** (2012) 16.
[13] Lu X. Z., Whangbo M.-H., Dong S., Gong X. G. and Xiang H. J., *Phys. Rev. Lett.*, **108** (2012) 187204.
[14] Dong S., Yu R., Liu J.-M. and Dagotto E., *Phys. Rev. Lett.*, **103** (2009) 107204.
[15] Bochu B., Chenavas J., Joubert J. C. and Marezio M., *Solid State Commun.*, **36** (1980) 133.
[16] Kresse G. and Hafner J., *Phys. Rev. B*, **47** (1993) R558.
[17] Kresse G. and Furthmüller J., *Phys. Rev. B*, **54** (1996) 11169.
[18] Perdew J. P., Burke K. and Ernzerhof M., *Phys. Rev. Lett.*, **77** (1996) 3865.
[19] Blöchl P. E., *Phys. Rev. B*, **50** (1994) 17953; Kresse G. and Joubert D., *Phys. Rev. B*, **59** (1999) 1758.
[20] Vasilev A. N. and Volkova O. S., *Low Temp. Phys.*, **33** (2007) 895.
[21] Chioncel L., Katsnelson M. I., de Groot R. A. and Lichtenstein A. I., *Phys. Rev. B*, **68** (2003) 144425.
[22] Malashevich A. and Vanderbilt D., *Phys. Rev. B*, **80** (2009) 224407.
[23] Ramirez A. P., *J. Phys.: Condens. Matter*, **39** (1997) 8171.
[24] Perks N. J., Johnson R. D., Martin C., Chapon L. C. and Radaelli P. G., *Nat. Commun.*, **3** (2013) 1277.
[25] Resta R., *Rev. Mod. Phys.*, **66** (1994) 899.
[26] Walker H. C., Fabrizi F., Paolasini L., de Bergevin F., Herrero-Martin J., Boothroyd A. T., Prabhakaran D. and McMorrow D. F., *Science*, **333** (2011) 1273.
[27] Dong S. and Liu J.-M., *Mod. Phys. Lett. B*, **26** (2012) 1230004.
[28] Xiang H. J., Wei S.-H., Whangbo M.-H. and Silva J. L. F. D., *Phys. Rev. Lett.*, **101** (2008) 037209.